

# Parameter Estimation of Frequency Modulated Continuous Wave (FMCW) Radar Signal using Wigner-Ville Distribution and Radon Transform

Sudhir Kumar<sup>1</sup>, Avinash Kumar Dubey<sup>2</sup>

Department of Electronics and Communication Engineering, Thapar University<sup>1,2</sup>

**Abstract:** In this study a time-frequency method based on Wigner-Ville Distribution (WVD) is used for detection and parameter estimation of Frequency Modulated Continuous Wave (FM-CW) Radar Signal. The proposed method uses the Pseudo-Wigner-Ville Distribution (PWVD) as a time-frequency detection technique and Radon Transform to identify the parameter of the modulation. The Wigner-Ville Radon Transform (WVRT) is suboptimal in detection and parameter estimation of FM-CW low probability of intercept (LPI) radar waveform. Autonomously detecting and analysing of FM-CW can eliminate the need of human intervention. It has been shown that the proposed algorithm can extract FM-CW radar modulation parameter efficiently.

**Keywords:** Wigner-Ville Distribution, Radon Transform, Modulation Parameters.

## I. INTRODUCTION

Threat against high power pulsed radar has increased due to advance in electronic support system. Radar system needs to be invisible and exploit low probability of intercept (LPI) signal to survive. These types of radar are generally known as LPI radar [1, 2]. Integration capabilities are able to detect and analyse LPI radar modulation.

LPI radar uses different modulation technique including FM-CW, phase shift keying (PSK), frequency shift keying (FSK) and hybrid FSK/PSK codes. FM-CW modulation technique is used in this paper. Various signal processing techniques have been investigated for the detection and estimation of LPI radar signals [3]. Time-frequency analysis is an efficient tool to analyse the behaviour of non-stationary waveforms.

By use of frequency spectrum technique we can only estimate which frequency components exist in the signal. By time-frequency analysis, it is possible to see which frequency component exist at a given time instant. Common methods used in time-frequency analysis are Short Time Fourier Transform (STFT), Choi-William Distribution (CWD) and Quadrature Mirror Filter Banks [7]. These methods have their advantages and disadvantages, such as STFT algorithm is easy to implement but it can only some simple modulation features. WVD could overcome STFT's disadvantages. WVD gives the highest energy concentration in time-frequency plane [2]. Its disadvantages are the negative and cross interference in the multi signal environment. WVD of FM-CW signal is shown in Figure 1. That shows the FM-CW component of received signal with cross-terms. The cross-term of signal is real, mixing with self-terms, and the amplitude is 2 times of self-terms, moreover, the cross-term is oscillatory type each two components can produce a cross-term [1].

Pattern recognition technique such as Hough Transform (HT) and Radon Transform (RT) are available for

autonomous detection and estimation of FM-CW radar's modulation parameter automatically.

Wigner-Ville Radon Transform (WVRT), the Radon transform of WVD is used in this paper for detection and estimation of FM-CW radar. Automate detection and estimation can eliminate the need of an operator [7].

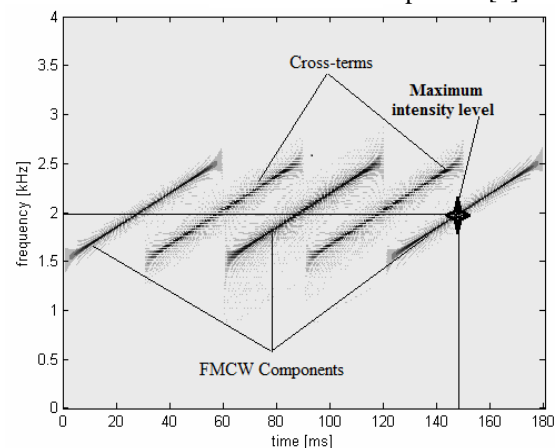


Figure 1. Wigner Ville distribution

## II. FREQUENCY MODULATED CONTINUOUS WAVE (FMCW) SIGNAL

FM-CW signal is the most important and common waveform structure used to achieve low probability of intercept functionality. FM-CW signal consists of positive and negative slopes. The modulating waveform for up ramp and down ramp is modelled as [5, 6].

$$f(t, u) = F_c \pm \frac{\Delta F}{2} \mp \frac{\Delta F}{t_m} t \quad (1)$$

$$t < 0 < t_m, t = 0 \text{ otherwise}$$

where  $F_c$  is the carrier frequency,  $\Delta F$  is modulation bandwidth and  $t_m$  is the modulation period,  $\Delta F$  is defined as

$$\Delta R = \frac{c}{2\Delta F} \quad (2)$$

where  $\Delta R$  is the range resolution.

The transmit signal for up ramp and down ramp is  $s(t, u)$   
 $= A_0 \cos \left( 2\pi \left( \left( F_c \pm \frac{\Delta F}{2} \right) t \mp \frac{\Delta F}{2t_m} t^2 \right) \right)$  (3)

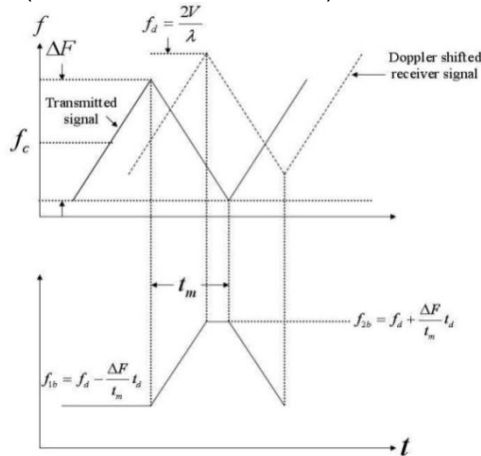


Figure 2. FMCW Signal and Doppler Shifted Return signal

Here  $f_{1b}$  and  $f_{2b}$  are the beat frequency for the first and second segment respectively,  $t_d$  is the round-trip delay time and  $f_d$  is the Doppler frequency.

### III. WIGNER-VILLE DISTRIBUTION

WVD is the most prominent member of time-frequency energy density function. WVD belongs to a more general distribution class, known as Cohen's class [2]. It possesses a great number of good properties and is a good method for non-stationary signal analysis. It could also reflect the frequency of the target radar return trend very well [2]. To obtain WVD, present and previous samples of the signal are multiplied. Fourier transform of these multiplications are calculated and then stacked in a WVD matrix. WVD produces cross-terms between every signal component pairs; these cross-terms limit the application of WVD method.

WVD of a continuous time signal  $x(t)$  is defined as [2]

$$W(t, \omega) = \int_{-\infty}^{\infty} x \left( t + \frac{\tau}{2} \right) x^* \left( t - \frac{\tau}{2} \right) e^{-i\omega\tau} d\tau$$
 (4)

$x(l)$  is a digital signal with  $l$  discrete time index between  $[-\infty, \infty]$ , discrete WVD is defined as [1]

$$W(l, \omega) = 2 \sum_{-\infty}^{\infty} x(l+n)x^*(l-n) e^{-2j\omega n}$$
 (5)

PWVD is derived by windowing the signal samples and defined as [1]

$$W(l, \omega) = 2 \sum_{n=-N+1}^{N-1} x(l+n)x^*(l-n) w(n)w(-n) e^{-2j\omega n}$$
 (6)

is a real valued window with length  $2N-1$  and  $w(0) = 1$ .

### IV. RADON TRANSFORM

The Radon Transform is the projection of the image intensity along a radial line oriented at a specific angle. It transforms the image with time-frequency domain into parameter  $(r, \theta)$  domain [3].

where  $\rho$  is the smallest distance from the origin and  $\theta$  is its angle with the x-axis.

A line is defined as

$$\rho = x \cos \theta + y \sin \theta$$
 (7)

Using this, the Radon transform of a 2-D image is

$$R(\rho, \theta) = \int_{-\infty}^{\infty} f(\rho \cos \theta - s \sin \theta, \rho \sin \theta + s \cos \theta) ds$$
 (8)

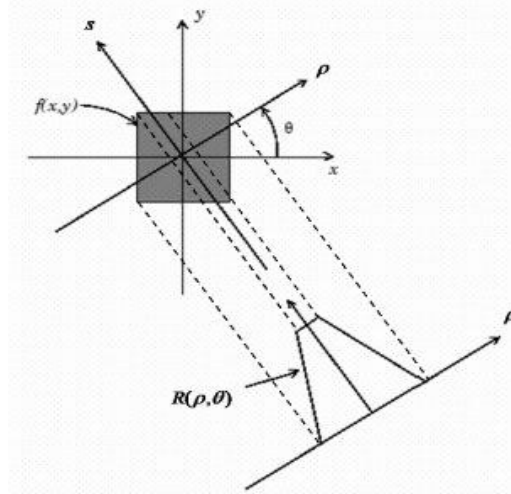


Figure 3. Geometry of the Radon Transform

where, the  $s$ -axis lies along the line perpendicular to  $\rho$  as shown in Figure 3. Here  $s$  can be calculated as

$$s = y \cos \theta - x \sin \theta$$
 (9)

$\rho$  and  $s$  can be calculated from  $x, y$  and  $\theta$  [12]. In this work, the projections of the images are computed as line integral from multiple source along parallel paths in a certain direction.

### V. METHOD

The first step is to compute the WVD of FM-CW Signal. The carrier frequency  $F_c$  is then extracted by finding the location of the maximum intensity level within the PWVD image as shown in Figure 1. In order to extract the code length  $T$  and bandwidth  $B$ , the Radon transform is computed from the time-frequency PWVD image.

#### 5.1. WIGNER RADON TRANSFORM

In this paper different type of LFM signals are investigated. Noise added with the signal is AWGN white Gaussian noise. When the signal is received from target noise is added from the environment that noise is AWGN Gaussian noise. AWGN white Gaussian noise of -3dB mixed with the FM-CW signal is shown in the Figure 4.

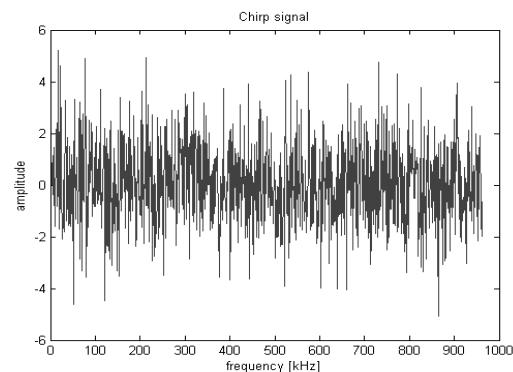


Figure 4. FM-CW with noise

The carrier frequency of FM-CW is directly determined from the PWVD image. Maximum intensity level in

PWVD image of FM-CW occurs at a point corresponding to carrier frequency. WVD of FM-CW is shown in figure 1.

Figure 5 shows the Gray-scale image from the PWVD illustrating the parameters to be extracted i.e., signal bandwidth  $B$  and code period  $T$ . In order to extract the code length  $T$  and bandwidth  $B$ , the Radon transform is computed from the time-frequency PWVD image. Radon transform finds  $\theta_0$  and  $d$ . Here  $d$  is the perpendicular distance in pixels between two consecutive linear energy lines at the modulation angle  $\theta_0$  [11].

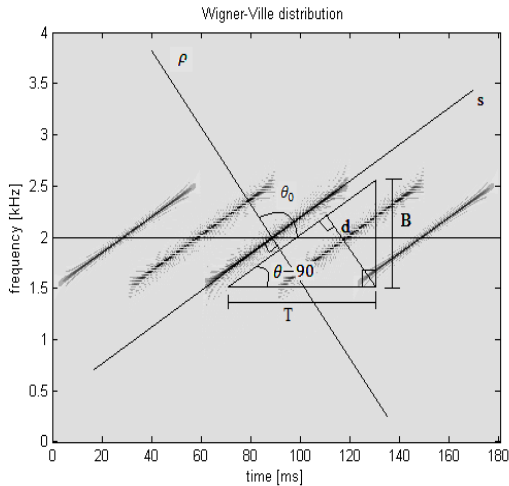


Figure 5. Radon Transform Geometry on PWVD

Once  $\theta_0$  and  $d$  are determined,  $B$  and  $T$  can be calculated using geometrical relations [11]. The Radon transform is implemented so that the parallelbeam projections of the image are taken between  $[0^0$  and  $90^0]$ .

Once the transform is completed it is normalized. In some cases the maximum intensity on the transform may occur around  $\theta = 90^0$  which corresponds to the marginal Frequency distribution (MFD) and around  $\theta = 0^0$  which corresponds to the time marginal.

In order to avoid the detection of the angle corresponding to the MFD and marginal time distribution, we assume that the slopes of linear energy lines are not between  $[5^0, -5^0]$  or between  $[85^0, 95^0]$ .

The projections on angles between  $\theta = [80^0, 100^0]$ ,  $[0^0, 5^0]$ ,  $[175^0, 179^0]$  are masked, and set to zero. After masking, the location of the maximum intensity level of the transform is found [11].

The coordinates of maximum level in Radon transform image corresponds to FM-CW components in WVD image is shown in Figure 6. Rho ( $\rho$ ) and Theta ( $\theta_0$ ) value are found by locating the maximum value in Radon transform.

Once  $\theta_0$  is found the projection at angle  $\theta_0$  is cropped from the masked Radon transform and a projection vector is obtained. Figure 7 illustrates the cropping of the projection vector at angle  $\theta_0$  form the masked Radon transform of FM-CW signal.

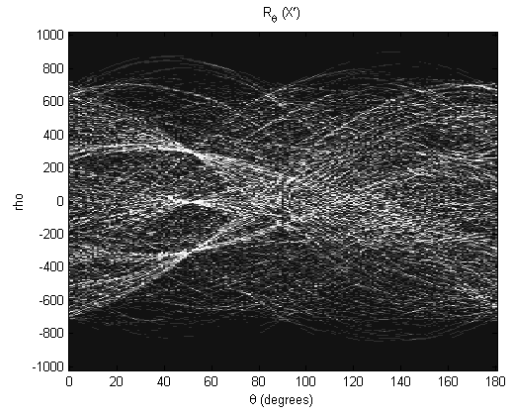


Figure 6. Radon Transform

From Figure 7 the number of FM-CW energy lines contained in the PWVD can easily be detected from both the Radon transform and the projection vector at angle  $\theta_0$ . The ripples between each FM-CW component correspond to the additive noise and the cross-term integration at angle  $\theta_0$ . The projection vector is then smoothed with a Wiener filter.

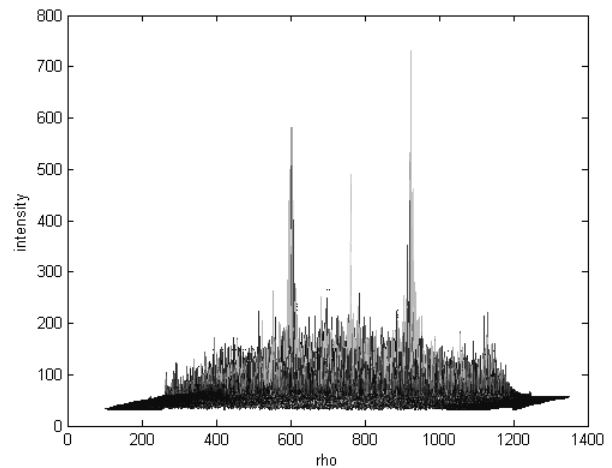


Figure 7. Projection cropping on the angle  $\theta_0$

After filtering, the projection vector is thresholded with a threshold equal to one half of the maximum value of the projection vector shown in Figure 8.

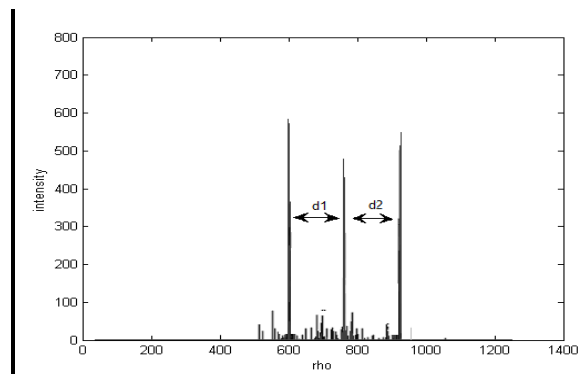


Figure 8. Filtered projection vector at angle  $\theta_0$

Heuristic threshold is used here to eliminate the peak representing the cross-term created by WVD. After thresholding distance can be found between the nonzero

values in the projection vector which correspond to the FM-CW energy components.

Once  $\theta_0$  and  $d$  are calculated as defined above, the remaining parameters are derived by using the geometric relations given in Figure 5 [11]. Bandwidth  $B$  can be calculated as [11]

$$B = \frac{\Delta f \left( \frac{d}{\cos \theta_0} \right)}{\tan \theta_0} \quad (10)$$

and the Modulation period  $T$  can be calculated as

$$T = \frac{1}{F_s} \left( \frac{d}{\cos \theta_0} \right) \quad (11)$$

where,  $\Delta f$  is the frequency resolution,  $F_s$  is the sampling frequency,  $d$  is distance between maximum intensity levels. Modulation bandwidth and modulation period are dependent on the distance ( $d$ ) between the maximum peaks. Therefore the correct value of  $d$  affects the parameter of the algorithm.

## VI. RESULT

The proposed algorithm is tested with different FM-CW signal with different parameter. The signal and parameters are presented in table 1.

Signal	$f_c$ (Hz)	$B$ (Hz)	$T$ (s)
$f_1$	2000	1120	0.060
$f_2$	1850	1380	0.040
$f_3$	1280	720	0.080

TABLE 1. Parameter of test signal

The simulation results showed that the algorithm proved well with low SNR levels (Table 2). The error between the extracted parameters and the true values were relatively too small providing high accuracy rates in average. If  $V_E$  is the extracted value and  $V_T$  is the true value, the absolute value of the relative error  $E_R$  is defined as [2]

$$E_R = \left| \frac{V_E - V_T}{V_T} \right| \quad (12)$$

Signal	SNR (dB)	Extracted parameter			Error percentage		
		$F_c$ (Hz)	$B$ (Hz)	$T$ (s)	$F_c$ -err	$B$ -err	$T$ -err
$F_1$	0	2001	1121	0.0603	0.50	0.089	0.5
$F_2$	0	1853	1383	0.0401	0.16	0.21	0.25
$F_3$	0	1283	723	0.0803	0.23	0.41	0.37
$F_1$	-3	2009	1123	0.0603	0.45	0.26	0.5
$F_2$	-3	1863	1387	0.0399	0.70	0.50	0.25
$F_3$	-3	1289	727	0.0796	0.70	0.97	0.5
$F_1$	-6	2021	1137	0.0604	1.05	1.51	0.66
$F_2$	-6	1870	1393	0.0403	1.08	0.94	0.87
$F_3$	-6	1297	736	0.0806	1.32	2.22	0.77

Table 2. Parameter extracted by WRT

### Relative error rate

The carrier frequency errors are very small for 0 dB but for -6 dB higher errors occur as shown in table 2. If frequency resolution of the PWVD is increased, the error in estimating  $F_c$  decreases. Note that advantage of approach is that the extraction algorithm is not affected from the cross-terms present within the PWVD images.

The reason is that integration of the cross-term projections is very small compared to the modulation projections [2].

## VII. CONCLUSIONS

In this paper FM-CW signal detection techniques was investigated. The architecture contained time-frequency detection techniques which provide image outputs of FM-CW radar waveforms. The use of time-frequency detection techniques provides an efficient method for the extraction of a composite feature vector to classify FM-CW Signals. An image cropping and feature extraction algorithm based on Radon transform was applied to the time-frequency images.

In order to enhance the feature extraction and algorithm and to increase its robustness and reliability, there are still some issues that should be addressed. Future efforts may include expanding the database of FM-CW radar modulations. The optimization process might be conducted in more detail. Other feature extraction methods might be investigated such as Fisher Linear Discriminant Analysis which might improve the extraction of class discriminating information better.

## REFERENCES

- [1] L. Cohen, "Time-Frequency distribution-A review," Proceedings of the IEEE, vol. 77, pp. 941-981, 1989.
- [2] P. E. Pace, Detecting and Classifying Low Probability of Intercept Radar, Norwood, MA: Artech House, 2004.
- [3] M. R. Hejazi, G. Shevlyakov, Y. S. Ho, "Modified discrete radon transform and their application to rotation-invariant image analysis," IEEE 8<sup>th</sup> Workshop on Multimedia Signal Processing, pp. 429-434, 2006.
- [4] S. O. Piper, "Homodyne FMCW radar range resolution effects with sinusoidal nonlinearities in the frequency sweep," Record of the IEEE International Radar Conference, pp. 563-567, 1995.
- [5] T. Claesen, W. Meckienbrauker, "Time-Frequency Signal Analysis by means of the Wigner Distribution," IEEE International Conference on Acoustics, Speech and Signal Processing, pp. 69-72, 1981.
- [6] J. C. Cexus, A. O. Boudraa, A. Bouchikhi, "A combined Teager-Huang and Hough Transform for LFM signal Detection," Proceedings of 4<sup>th</sup> International Symposium on Communications, Control and signal processing, Limassoi, 2010.
- [7] J. C. Cexus, A. O. Boudraa, A. Bouchikhi, "A combined Teager-Huang and Hough Transform for LFM signal Detection," Proceedings of 4<sup>th</sup> International Symposium on Communications, Control and signal processing, Limassoi, 2010.
- [8] T. Farrel, and G. Prescott, "Anine-tile algorithm for LPI signal detection using QMF filter bank trees," Proceedings of the IEEE Conference on Military Communication, vol. 3, pp. 974-978, 1996.
- [9] M. Brandt-Pearce, "Detection and Estimation of LFMCW Radar Signals," IEEE Transactions on Aerospace and Electronic Systems, vol. 48, no.1, pp. 405-418, 2012.
- [10] M. Mesbah, B. Boashash, "A Discrete Time-Frequency Wigner-Ville Distribution: Properties and Implementation," Signal Processing Research Laboratory, Brisbane, Australia, 2007.
- [11] T. O. Gulum, A. Y. Erdogan, T. Yildirim, "Parameter Extraction of FMCW Modulated Radar Signals using Wigner-Hough Transform," IEEE 12<sup>th</sup> international symposium on Digital Object Identifier, pp. 465-468, 2011.
- [12] T. O. Gulum, "Autonomous Nonlinear Classification of LPI Radar Signal Modulations," Naval Postgraduate School Master's Thesis, 2007.
- [13] M. Wang, A. K. Chan, C. K. Chui, "Linear frequency modulated signal detection using Radon-ambiguity transform," IEEE Transactions on Signal Processing, vol. 26, no. 3, pp. 571-586, 1998.